Surface Plasmon Resonance of Au Colloid-Modified Au Films: Particle Size Dependence

L. Andrew Lyon, David J. Peña, and Michael J. Natan*

Department of Chemistry, The Pennsylvania State University, University Park, Pennsylvania 16802

Received: December 14, 1998; In Final Form: May 12, 1999

The influence of colloid diameter on the surface plasmon resonance (SPR) response of a colloidal Au modified Au film is described. Adsorption of 30−59 nm diameter colloidal Au on the surface of a 47 nm thick Au film results in dramatic, size-dependent shifts in plasmon angle, minimum reflectance, and curve breadth. Each of these parameters is observed to increase with particle diameter and particle coverage, eventually reaching a plateau when the attenuation of the SPR curve is maximized. The angle of maximum change in reflectance is observed to be independent of particle size; thus, the reflectance at that angle is proposed as a method for quantifying the perturbation induced by a particular size and coverage of colloidal Au. These results are discussed in terms of the detection limits and dynamic range of colloidal Au-amplified SPR biosensing.

Introduction

We describe herein the effect of Au colloid diameter and coverage on colloidal Au amplified surface plasmon resonance (SPR) response of thin Au films.[1] Surface plasmon resonance has recently gained in popularity as a general technique for the study of chemical interactions occurring at the surface of thin metal films.[2] While the technique has been demonstrated to have utility in the investigations of many different chemistries,[3] much of the recent activity has focused on problems in biochemistry,[4] including protein−protein[4] and DNA−DNA[5] interactions. The physical basis for SPR sensing relies on the ability of the technique to resolve small changes in refractive index near a metal/solution interface.[6] Interactions between a surface-confined biomolecule and a solution-borne species result in such changes; the biomolecular recognition event then is manifested as a measurable change in the angle-dependent reflectance of the metal film. This type of SPR sensing is typically carried out on a commercial instrument that uses a carboxylated dextran gel on a Au film as the sensor surface, where the gel acts as a host for the surface-confined binding partner.[7] However, the generality of the technique has led to its implementation in a number of other formats, including imaging,[8] microscopy,[9] holography,[10] and fiber optic[11] and miniaturized sensors.[12] Other analytical techniques have also been coupled to SPR, including mass spectrometry[13] and Raman scattering.[14] More advanced optical immunosensor architectures have also been explored; most notable are reports of amplified biosensing where the coupling of large particles (liposomes[15] and colloidal nanoparticles[1,16]) to biomolecules can in turn cause large refractive index shifts during the biomolecular recognition event. We have recently reported a similar approach wherein colloidal Au was employed as a biocompatible, high refractive index tag in a protein in a sandwich immunoassay.[1] In this work, a conjugate between a monoclonal antibody and a 12 nm colloidal Au particle produced a greater than 20-fold increase in plasmon angle shift over that observed in an assay using the unlabeled antibody. This result, combined with previous reports of the preparation of sols of colloidal Au over a wide range of sizes (2−100 nm in diameter),[17] and the preparation of biocompatible arrays of such particles[18] has led us to investigate the SPR of colloid-modified Au films as a function of particle size. Despite the fact that large colloidal particles are typically nonideal as tags for real-time bioanalysis due to slow diffusion kinetics, steric hindrance (at high surface coverage), and an increased opportunity for multivalent binding, it was reasoned that they would be excellent as tags for the determination of extremely low quantities of analyte that are not routinely observable using traditional assay methodologies. Accordingly, we find that, as the colloid diameter is increased, the perturbation of the SPR curve becomes much more significant. A direct, unambiguous correlation between the changes in the SPR curve and colloid size and coverage can then be made by carefully counting the surface-bound particles via atomic force microscopy. This ability to independently measure the analyte surface coverage is an improvement over the traditional method of inferring analyte surface concentrations from shifts in the SPR plasmon angle. Indeed, the observed SPR curves (reflectance versus angle) are attenuated to such a large degree that the perturbation cannot be sufficiently described by the plasmon angle shift alone. Differential curves are therefore used to determine the angle of maximum reflectance change, which is in turn used to describe the effect of each particle size and coverage. These results demonstrate the potential for significant improvement in the sensitivity and dynamic range of colloidal Au amplified biosensing by increasing the size of the colloidal tag.

Experimental Section

Reagents. All reagents were used as received without further purification. H_2O was purified to >18 MW with a Barnstead Nanopure system and filtered through a 200 mm particulate filter. 3-Mercaptopropyltrimethoxysilane was purchased from United Chemical Technologies and stored in a vacuum desiccator until just prior to use. CH_3CH_2OH was purchased from Pharmco. 2-Mercaptoethylamine (MEA) was purchased from Sigma. Citric acid trisodium salt was purchased from Aldrich. $HAuCl_4$ was from Acros. HNO_3, HCl, NaOH, CH_3OH, and H_2SO_4 were from EM Science.

Colloidal Au Preparation. Colloidal Au of mean diameter <15 nm was prepared by citrate reduction of $HAuCl_4$ as reported previously.[19] Larger Au colloid was prepared using a modified

* To whom correspondence should be addressed. E-mail: natan@chem.psu.edu.

10.1021/jp984739v CCC: $18.00
Published on Web 06/25/1999

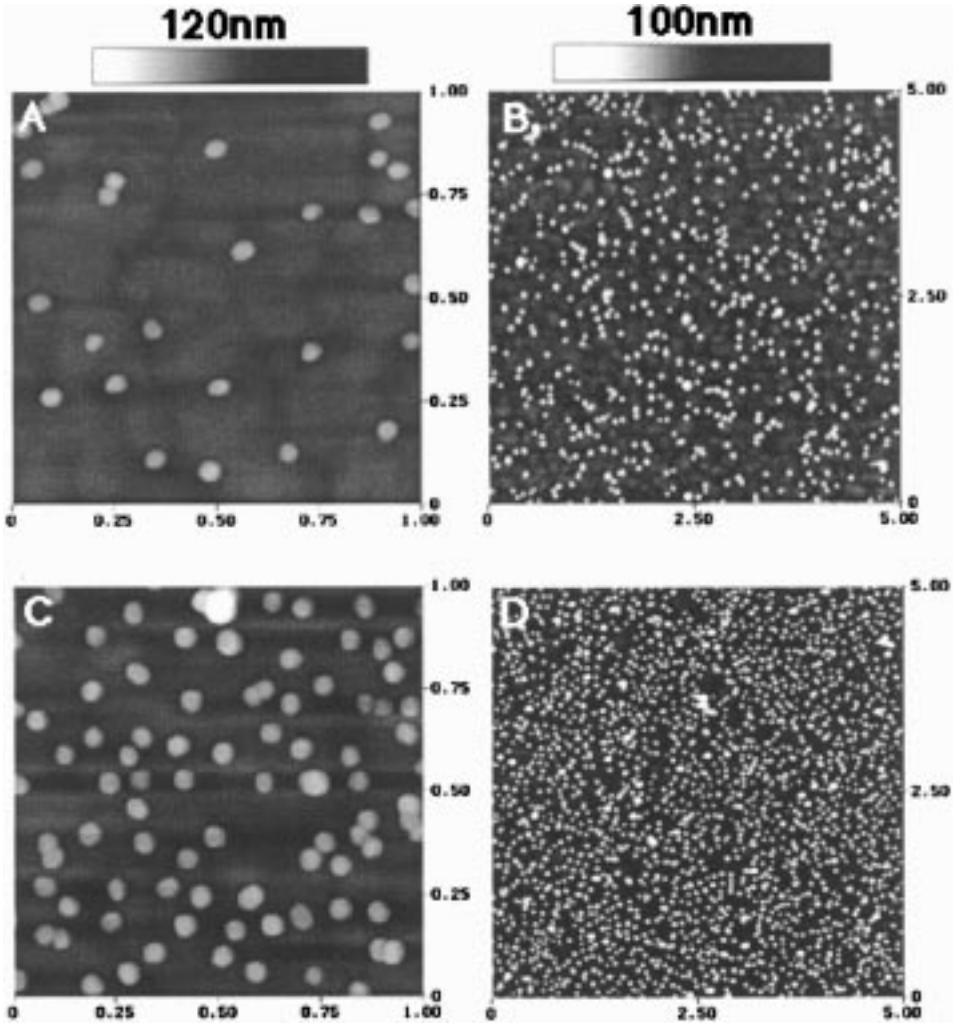

Figure 1. Representative 1 μm × 1 μm (A,C) and 5 μm × 5 μm (B,D) TM-AFM images of 30 nm diameter colloidal Au immobilized on evaporated Au. Colloid exposure times were 30 min (A,B) and 90 min (C,D). Vertical scale bars are 120 nm for panels A and C and 100 nm for panels B and D, as indicated.

"seed colloid" technique.[17] 12 nm colloid (major axis 12 nm ± 2 nm and minor axis 11 nm ± 1 nm from 758 particles sized) in an amount of 1 mL was used as the starting material, with 100 mL 0.01% $HAuCl_4$ and 500 mL of 38.8 mM citrate solution. The resulting sample as analyzed by TEM showed a major axis of 45 nm ± 5 nm and a minor axis of 37 nm ± 4 nm from 274 particles sampled. A second batch of large colloid produced using 100 mL of 0.02% $HAuCl_4$ and 1.0 mL of 38.8 mM citrate solution showed a major axis of 59 nm ± 14 nm and a minor axis of 52 nm ± 11 nm from 424 particles. Similar protocols produced batches of particles of the following dimensions: 30 nm ± 3 nm (major axis) × 25 nm ± 2 nm (minor axis) from 373 particles sized and 35 nm ± 3 (major axis) × 30 ± 3 nm (minor axis) from 112 particles sized. These preparations used 100 mL of 0.01% $HAuCl_4$ and 500 mL of 38.8 mM citrate solution with 3 mL and 2 mL of 12 nm diameter colloidal "seed" added, respectively. Average particle diameter and standard deviations were determined by particle size analysis of TEM images (Supporting Information) using NIH Image v. 1.62 software.[20]

Au Film Preparation. Thin (47−50 nm) Au films were prepared by thermal evaporation of Au shot (99.95%, Johnson Mathey) from a resistively heated molybdenum boat (Kurt J. Lesker) in a diffusion-pumped Edwards Auto 306 thin film fabrication system. Evaporation substrates were Fisherbrand 1" × 1" coverslips. Prior to evaporation, the substrates were treated with a 10% (v/v) 3-mercaptopropyltrimethoxysilane/CH_3OH solution for 30 min in order to increase the adhesion of Au to the glass.[21] Au was deposited at a pressure of ∼1 × 10−6 mbar at 0.3−0.4 nm/s with constant sample rotation to ensure uniform deposition. Following evaporation, the films were annealed in a home-built oven at 300 °C for 5−10 min under a constant flow of Ar to decrease the surface roughness of the evaporated layer.

Atomic Force Microscopy and Particle Counting. Tapping mode atomic force microscopy (TM-AFM) images acquired were obtained using a Digital Instruments Nanoscope IIIA operated in tapping mode with an acquisition frequency of 1.5 Hz and line density of 512. Standard 200 mm etched silicon probes were used. For the purposes of coverage determination, at least four images were obtained from two distinct regions of each sample. Two 5 μm × 5 μm images were taken ∼0.5 mm apart to confirm that the coverage was homogeneous. At each position, 1 μm × 1 μm scans were captured in order to obtain higher resolution images. Representative images of surfaces modified with 30 nm diameter colloidal Au are shown in Figure 1. Images A and B are the result of a 30 min exposure to colloidal Au, while images C and D result from exposure to a sol for 90 min. Particle counting was done manually from captured images (images obtained for other particle sizes are available in Supporting Information). Reported numbers are average coverage values obtained from 2 to 3 images.

SPR Instrumentation. The SPR apparatus has been described in detail elsewhere.[1a] Briefly, excitation of the surface plasmon is accomplished using the Kretschmann geometry where a 1" diameter hemispherical prism (BK7 glass, Esco-products) is index matched (Zeiss immersion oil, $n = 1.515$) to a glass substrate onto which Au had been previously evaporated. The SPR excitation source is a HeNe laser (632.8 nm, 5 mW maximum power, Melles Griot). The beam is focused onto the prism/sample assembly, and the reflected beam is then detected at a silicon photodiode detector (Thor Labs). Angular positioning of the sample is accomplished with a home-built $\theta-2\theta$ stage consisting of two high-resolution (0.001°) servo-drive rotation stages (Newport) that are mounted together such that their axes of rotation are collinear. The prism/sample assembly is then mounted on the $\theta-2\theta$ stage such that the center of the prism/sample assembly is at the axis of rotation. Stage rotation and data collection are controlled through a computer interface that was developed in-house with the LabVIEW programming language (v. 4.01, National Instruments).

Au Film Derivatization. Annealed Au films were modified with MEA from a 1.0 mM ethanolic solution for a period of 30 min. Longer immersion times did not noticeably improve the efficiency or density of subsequent derivitization steps. Immobilization of colloidal Au onto amine-modified (MEA-coated) surfaces was performed from aqueous sols (concentration = 0.17 nM) at room temperature on an orbital shaker. Amine-modified surfaces induce the strong adsorption of colloidal Au particles by virtue of the availability of an electron lone pair on the amine nitrogen, as well as ionic interactions with the negatively charged particles. Previous studies have investigated these interactions, as well as those occurring with −SH, −CN, and −COOH functionalized surfaces.[18] In all experiments, care was taken to ensure that the identical region of a particular sample was interrogated with both SPR and AFM. Accordingly, a box was scratched around the area illuminated during the SPR experiment. The colloid coverage within that area was then measured via AFM, thereby alleviating any errors due to uneven surface derivatization over large length scales. It is important to note that the solution agitation is an important step in obtaining particle-diameter-independent coverage values. At short exposure times (<1 h) and identical solution particle concentrations, approximately equal particle surface concentrations may be obtained independent of colloid diameter (Supporting Information). This removes the diffusion dependence of surface attachment and leaves the sticking probability (which is only slightly influenced by particle diameter) as the determining factor in the resultant particle number density.

Results and Discussion

Our initial work on the SPR of colloid-modified Au films revealed a significant attenuation of plasmon propagation as a function of 12 nm diameter colloidal Au coverage while also identifying a dependence on particle size.[1a,b] However, a detailed description of the coverage-dependent SPR response due to the adsorption of larger colloidal particles has not been described. To understand the influence of colloid size and coverage on the observed SPR reflectance, we have explored this phenomenon in a more detailed fashion. Figure 2 shows the SPR curves for 47 nm thick Au films that were subsequently modified with similar number densities ($1.3 \pm 0.15 \times 10^9$ particles/cm^2) of 30, 35, 45, and 59 nm diameter colloidal Au. Despite this relatively low number density, the SPR curve changes dramatically with particle size, as the minimum reflectance increases from 10% to 35% over a less than 2-fold increase in diameter

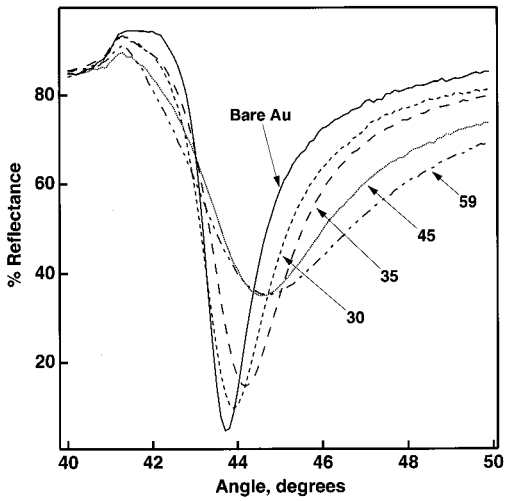

Figure 2. SPR curves (reflectance vs angle) of a 47 nm thick Au film coated with 2-mercaptoethylamine (—) and a submonolayer of colloidal Au ($1.3 \pm 0.15 \times 10^9$ particles/cm^2). Particle diameters are 30 (- - -), 35 (— — —), 45 (•••), and 59 nm (— - - —).

(30 to 59 nm). Indeed, for the largest particle size (59 nm), the SPR curve bears little resemblance to that of a bare evaporated film; the curve is very shallow and broad, without the well defined plasmon angle that is typically observed in SPR. Another parameter that is changing in the data shown in Figure 2 is the ellipticity of the particles. As described above, increasing the particle size serves to increase the particle ellipticity. This change in particle shape may alter the SPR response from that which would be obtained from ideal spherical particles. However, we currently have no reliable method or experimental guide for estimating the magnitude of this effect and will therefore describe the observed SPR curves in terms of particle diameter (major axis) only.

As described previously,[1a,22] these perturbations in the SPR curve are most likely the result of two processes, absorptive damping and localized coupling. Since the colloidal particles possess an imaginary component to their dielectric constant, there is a significant absorption cross section for the particulate layer. This should result in absorption of plasmon energy and hence damping of the surface mode.[6] Furthermore, colloidal particles may also act as localized defect or roughness sites on the metal surface. SPR shifts associated with scattering and absorption by surface roughness are well documented,[6c,22d] and it is likely that similar processes are responsible for at least a portion of the shifts observed here. It is interesting to note that while the number of colloidal particles per unit area is being held constant for the data shown in Figure 2, the fractional surface coverage is varying with particle size. In other words, an equal number of two different size particles will cover different geometric areas. Taking this into account, we find that the fractional coverage of 30, 35, 45, and 59 nm particles are 1.2, 1.6, 2.6, and 4.5% of a close packed monolayer, respectively. The above changes in the SPR response can therefore be broken down into contributions from four physical parameters of the colloidal particles. First, the per-particle extinction coefficient (absorption cross section) is known to depend roughly on the square of the particle radius for surface-confined particles addressed by an attenuated total reflectance technique.[23] Absorptive damping is therefore expected to scale in the same manner. Second, the fractional coverage (and hence, the total area of surface−colloid interaction) also increases as the square of the particle radius. Third, the thickness of the colloidal film (taken to be the geometric, not effective dielectric thickness) is

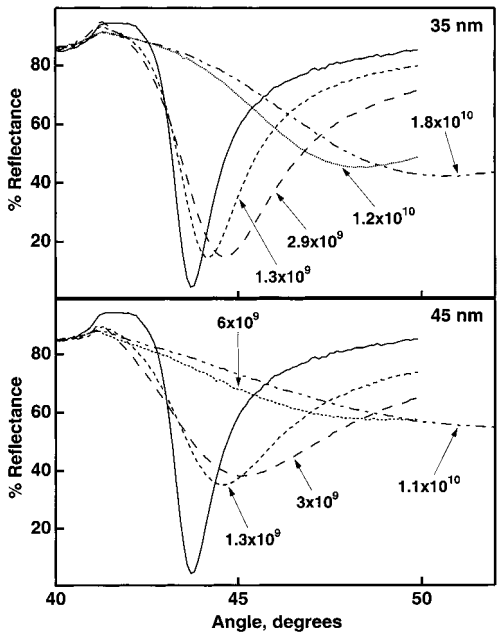

Figure 3. SPR curves (reflectance vs angle) of a 47 nm thick Au film coated with 2-mercaptoethylamine (—) and a layer of 35 nm diameter colloidal Au (top) and 45 nm diameter colloidal Au (bottom). Colloid surface concentrations (in particles/cm^2) are as labeled on the graph.

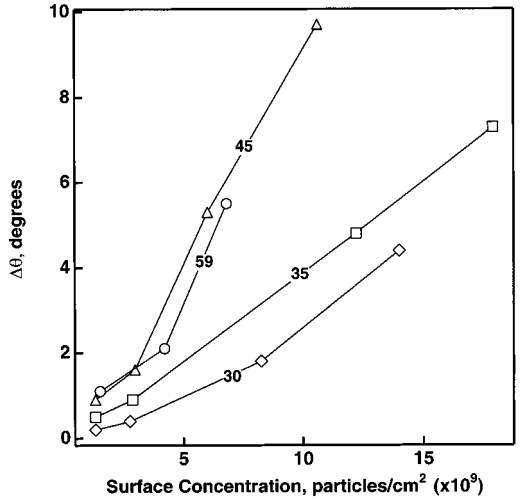

Figure 4. The plasmon angle shift plotted as a function of particle number density for 30 (- ◇ -), 35 (- □ -), 45 (- △ -), and 59 nm (- ○ -) diameter colloidal Au.

equal to the particle diameter; SPR is highly sensitive to the dimensions of the damping medium and should therefore be sensitive to the diameter of the particles.[6,24] Finally, the plasmon scattering induced by the particles should contribute to damping. As with absorption, the scattering efficiency scales with the cross-sectional area of the particle and hence the square of the radius.[25] An additional parameter not investigated here concerns the distance of the particle film from the Au surface. Presumably, a thicker SAM layer would serve to modulate the changes in the SPR curve. Previous studies of Ag island films spaced at specific distances away from a SPR-active surface have shown that the distance dependence is more complex than the simple exponential decrease of the plasmon electric field.[22e] Our current understanding of the damping mechanism does not yet allow for speculation as to the relative contributions from these parameters. Presumably, a more detailed theoretical description of particle−surface coupling would be necessary before quantitation of each factor is possible.

The basis of a particle-enhanced bioassay is that biomolecular interaction events lead to particle immobilization, i.e., more immobilized proteins yield higher particle coverage.[1a,b,16] Ideally, some SPR parameter will scale linearly with particle count to allow for a quantitative assay. In the vast majority of systems studied via SPR, the plasmon angle (angle of minimum reflectance) is monitored and correlated with the amount of immobilized material. Figure 3 shows the changes that occur in the SPR curve as a function of surface concentration for 35 nm (top panel) and 45 nm (bottom panel) diameter colloidal Au. In the case of 35 nm colloidal Au, a low number density of particles induces relatively small plasmon angle shifts and reflectance changes. As the number density is increased, changes in the position and the magnitude of minimum reflectance become larger, eventually attaining a total plasmon shift of ∼7° and a reflectance increase of >40%. Somewhat larger angle shifts are observed for 45 nm diameter colloid; the initial change in plasmon angle is significant and increases rapidly with increasing coverage. However, the curve shape evolves much more rapidly in the case of 45 nm colloid, as a >30% reflectance is observed at the lowest surface concentration. The trend is similar for other sizes of colloidal Au, as smaller perturbations are observed for 30 nm diameter Au and much larger initial reflectance changes are observed to occur due to 59 nm particles (Supporting Information).

From a practical standpoint, it is not the gross perturbation of the curve that is important in an SPR sensing format but rather the maximum change that can be observed in either the plasmon angle shift or in the reflectance. It is evident from the data shown in Figures 2 and 3 that, at higher coverage, the SPR curve becomes too broad for accurate plasmon angle determination. While it is desirable to know the plasmon angle (which can be directly correlated with changes in refractive index at the Au surface), we observe a deviation from linearity in plots of plasmon angle versus particle number density (Figure 4), suggesting that the traditional linear dependence of angle on the number of immobilized species does not necessarily hold for colloidal Au particles. Therefore, it is more practical from both an instrumental and a sensitivity standpoint to measure the reflectance change at a single angle, despite the fact that the reflectance change itself possesses no clear physical meaning in terms of the interfacial dielectric properties.

The maximum reflectance change can be determined easily by taking the difference between the SPR curves due to the modified film and the unmodified film. Figure 5 shows the difference curves calculated from the data shown in Figure 3. For both 35 and 45 nm particles, a peak is observed at ∼43.7°, suggesting that the minimum of the unperturbed SPR curve is the optimal observation angle for the coverages investigated here. The large size of reflectance changes observed here suggests that much lower surface concentrations may be detectable. Indeed, for 45 nm diameter particles, a number density of 1.3×10^9 particles/cm^2 results in a reflectance change of 40%. Since our current instrumentation is able to detect a change in reflectance of <0.1%, we should be able to detect a 400-fold lower particle coverage ($\sim 3 \times 10^6$ particles/cm^2, 0.0065% of a monolayer), assuming a linear SPR response at low coverage.

The maximum change in reflectance is plotted as a function of number density in Figure 6 for 35 and 45 nm diameter colloidal Au. For all particle diameters, the peak of the differential curve is approximately 43.7° (differential curves for 30 and 59 nm diameter particles are available in Supporting Information), again indicating that the ideal observation angle

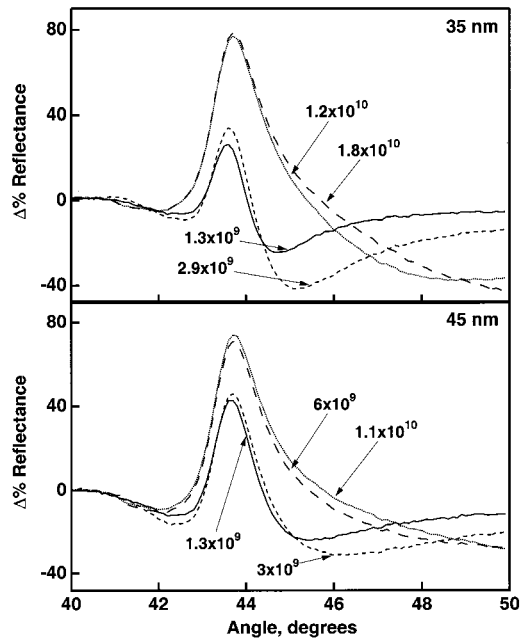

Figure 5. Differential SPR curves obtained by subtraction of the Au + MEA curve from each curve due to a 35 nm diameter (top) and 45 nm diameter (bottom) colloid-modified Au film. Colloid surface concentrations (in particles/cm^2) are as labeled on the graph.

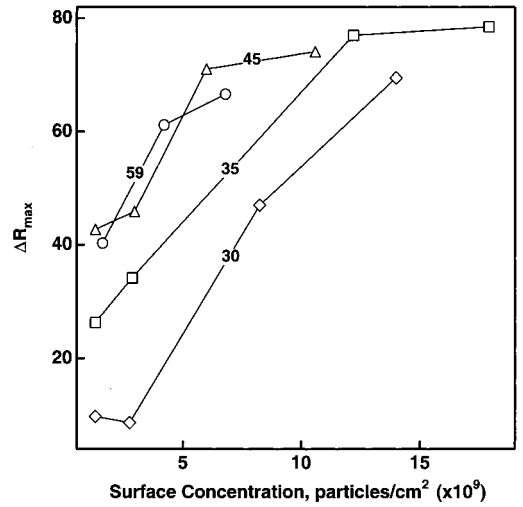

Figure 6. The maximum reflectance change plotted as a function of particle number density for 30 (- ◇ -), 35 (- □ -), 45 (- △ -), and 59 nm (- ○ -) diameter colloidal Au.

is the same, independent of particle size. In terms of assay and sensing applications, this is a distinct advantage of particle enhancement, as the angle where the largest signal will be observed can be known prior to performing an assay. This may in some cases eliminate the need for high-resolution scanning in order to determine the amount of immobilized material. Measurement of the percent reflectance at a specific angle may also be subject to less error, as determination of the absolute plasmon angle becomes difficult at higher particle coverage. However, one potential drawback to this analysis method exists in terms of the dynamic range of the particle-enhanced sensing motif. As the SPR curve shifts to higher angles, we observe a limit for the maximum reflectance at a particular angle. This is reflected by the plateaus in Figure 6 for the cases of 35 and 45 nm diameter particles. While increased particle surface concentrations induce further changes in the plasmon angle, the change in reflectance at any one angle becomes quite small due to the shallowness of the curves. This limitation can be thought of as a restricted dynamic range for particle enhancement, where the highest sensitivity and linearity may be obtained at low particle number density; larger numbers of immobilized particles result in a nonlinear response with respect to the percent reflectance. It is also apparent from both Figures 4 and 6 that 59 nm diameter colloidal particles do not serve to significantly change SPR response as compared to similar coverages of 45 nm diameter particles. This suggests that there is a point at which increasing the particle size ceases to improve the potential sensitivity of a particle-enhanced assay over the number densities studied here. Current efforts are focused on extending the range of particle number densities probed by SPR and extending the size dependence studies to both smaller and larger particles. Finally, we are attempting to develop a theoretical understanding of the factors influencing particle-induced plasmon damping.

Conclusions

The SPR response of a colloidal Au-modified 47 nm thick Au film has been measured as a function of particle size for 30−59 nm diameter particles. Large perturbations in the observed SPR curve are observed for all sizes, with the changes increasing in magnitude as the particle size is increased. The maximum induced reflectance change has been used as a method for quantifying the potential utility of a particular particle size for colloid-amplified biosensing. It is proposed that an increase in particle size leads to a decrease in both the detection limit and the maximum level of quantitation. This effectively shifts the theoretical window of detectable analyte concentrations to lower levels as the particle size is increased. Efforts currently underway are focused on investigating the utility of these particles in immunoassays and quantifying the actual detection limits as a function of particle size.

Acknowledgment. Support from NSF (CHE-9627338, DBI-9872629), NIH (GM55312-01), and the Alfred P. Sloan Foundation is gratefully acknowledged.

Supporting Information Available: A table and TEM images detailing the size and size dispersity of the colloidal particles, representative AFM images of the colloid-modified Au films, a plot of particle surface concentration versus exposure time, SPR curves of colloid-modified Au films and the resultant differential SPR curves. This material is available free of charge via the Internet at http://pubs.acs.org.

References and Notes

(1) (a) Lyon, L. A.; Musick, M. D.; Natan, M. J. *Anal. Chem.* **1998**, *70*, 5177−5183. (b) Lyon, L. A.; Musick, M. D.; Smith, P. C.; Reiss, B. D.; Peña, D. J.; Natan, M. J. *Sens. Actuators, B* **1999**, *54*, 118−124. (c) Lyon, L. A.; Holliway, W. D.; Natan, M. *J. Rev. Sci. Inst.* **1999**, *70*, 2076−2081.

(2) For recent reviews, see, for example: (a) Schuck, P. *Annu. Rev. Biophys. Biomol. Struct.* **1997**, *26*, 541−566. (b) Garland, P. B. *Quart. Rev. Biophys.* **1996**, *29* (1), 91−117. (c) Löfås, S. *Pure Appl. Chem.* **1995**, *67*, 829−834. (d) Frutos, A. G.; Corn, R. M. *Anal. Chem.* **1998**, *70*, 449A.

(3) (a) Hanken, D. G.; Corn, R. M. *Anal. Chem.* **1995**, *67*, 3767−3774. (b) Frey, B. L.; Jordan, C. E.; Kornguth, S.; Corn, R. M. *Anal. Chem.* **1995**, *67*, 4452−4457. (c) Mrksich, M.; Sigal, G. B.; Whitesides, G. M. *Langmuir* **1995**, *11*, 4383−4385. (d) Sigal, G. B.; Bamdad, C.; Barberix, A.; Strominger, J.; Whitesides, G. M. *Anal. Chem.* **1996**, *68*, 490−497.

(4) (a) Heyse, S.; Ernst, O. P.; Dienes, Z.; Hofmann, K. P.; Vogel, H. *Biochemistry* **1998**, *37*, 507−522. (b) Tung, J.-S.; Giminez, J.; Przysiecki, C. T.; Mark, G. *J. Pharm. Sci.* **1998**, *87*, 76−80. (c) Berger, C. E. H.; Beumer, T. A. M.; Kooyman, R. P. H.; Greve, J. *Anal. Chem.* **1998**, *70*, 703−706. (d) Li, J.; Cook, R.; Doyle, M. L.; Hensley, P.; McNulty, D. E.; Chaiken, I. *Proc. Nat. Acad. Sci.* **1997**, *94*, 6694−6699. (e) Autiero, M.; Gaubin, M.; Mani, J.-C.; Castejon, C.; Martin, M.; El Marhomy, S.; Guardiola, J.; Piatier-Tonneau, D. *Eur. J. Biochem.* **1997**, *245*, 208−213.

(f) Myszka, D. G.; Morton, T. A.; Doyle, M. L.; Chaiken, I. M. *Biophys. Chem.* **1997**, *64*, 127−137. (g) Lange, C.; Koch, K.-W. *Biochemistry* **1997**, *36*, 12019−12026. (h) Ladbury, J. E.; Lemmon, M. A.; Zhou, M.; Green, J.; Botfield, M. C.; Schlessinger, J. *Proc. Natl. Acad. Sci. U.S.A.* **1995**, *92*, 3199−3203. (i) Ward, L. D.; Howlett, G. J.; Hammacher, A.; Weinstock, J.; Yasukawa, K.; Simpson, R. J.; Winzor, D. J. *Biochemistry* **1995**, *34*, 2901−2907. (j) Minunni, M. *Anal. Lett.* **1995**, *28*, 933−944. (k) Bernard, A.; Bosshard, H. R. *Eur. J. Biochem.* **1995**, *230*, 416−423. (l) O'Brien, D. P.; Kemball-Cook, G.; Hutchinson, A. M.; Martin, D. M. A.; Johnson, D. J. D.; Byfield, P. G. H.; Takamiya, O.; Tuddenham, E. G. D.; McVey, J. H. *Biochemistry* **1994**, *33*, 14162−14169.

(5) (a) Peterlinz, K. A.; Georgiadis, R. M.; Herne, T. M.; Tarlov, M. J. *J. Am. Chem. Soc.* **1997**, *119*, 3401−3402. (b) Caruso, F.; Rodda, E.; Furlong, D. N.; Haring, V. *Sens. Actuators, B* **1997**, *41*, 189−197. (c) Bier, F. F.; Kleinjung, F.; Scheller, F. W. *Sens. Actuators, B* **1997**, *38*−*39*, 78−82.

(6) (a) Pockrand, I. *Surf. Sci.* **1978**, *72*, 577−588. (b) Economou, E. N. *Phys. Rev.* **1969**, *182*, 539−554. (c) *Surface Plasmons on Smooth and Rough Surfaces and on Gratings*; Raether, H., Ed.; Springer Tracts in Modern Physics, Vol. 111; Springer-Verlag: Berlin, 1988. (d) Hansen, W. N. *J. Opt. Soc. Am.* **1968**, *58*, 380−390.

(7) (a) Karlsson, R.; Fält, A. J. *Immunol. Methods* **1997**, *200*, 121−133. (b) Adamczyck, M.; Gebler, J. C.; Gunasekera, A. H.; Mattingly, P. G.; Pan, Y. *Bioconjugate Chem.* **1997**, *8*, 133−145. (c) Liedberg, B.; Lundström, I.; Stenberg, E. *Sens. Actuators, B* **1993**, *11*, 63−72. (d) Johne, B.; Gadnell, M.; Hansen, K. J. *Immunol. Methods* **1993**, *160*, 191−198. (e) O'Shannessy, D. J.; Brigham-Burke, M.; Soneson, K. K.; Hensley, P.; Brooks, I. *Anal. Biochem.* **1993**, *212*, 457−468. (f) Toyama, S.; Ikariyama, Y. *Chem. Lett.* **1997**, 1083−1084.

(8) (a) Jordan, C. E.; Corn, R. M. *Anal. Chem.* **1997**, *69*, 1449−1456. (b) Jordan, C. E.; Frutos, A. G.; Thiel, A. J.; Corn, R. M. *Anal. Chem.* **1997**, *69*, 4939−4947. (c) Thiel, A. J.; Frutos, A. G.; Jordan, C. E.; Corn, R. M.; Smith, L. M. *Anal. Chem.* **1997**, *69*, 4948−4956.

(9) (a) Hickel, W.; Kamp, D.; Knoll, W. *Nature* **1989**, *339*, 186. (b) Rothenhausler, B.; Knoll, W. *Nature* **1988**, *332*, 615−617. (c) Hickel, W.; Knoll, W. *J. Appl. Phys.* **1990**, *67*, 3572−3575. (d) Knobloch, H.; Knoll, W. *Makromol. Chem., Macromol. Symp.* **1991**, *46*, 389−393. (e) Flatgen, G.; Krischer, K.; Pettinger, B.; Doblhofer, K.; Junkes, H.; Ertl, G. *Science* **1995**, *269*, 668−671. (f) Kim, Y.-K.; Ketterson, J. B.; Morgan, D. J. *Opt. Lett.* **1996**, *21*, 165−167.

(10) Maruo, S.; Nakamura, O.; Kawata, S. *Appl. Opt.* **1997**, *36*, 2343−2346.

(11) (a) Jorgenson, R. C.; Yee, S. S. *Sens. Actuators, B* **1993**, *12*, 213−220. (b) Abdelghani, A.; Chovelon, J. M.; Jaffrezic-Renault, N.; Ronot-Troli, C.; Veillas, C.; Gagnaire, H. *Sens. Actuators, B* **1997**, *38*−*39*, 407−410. (c) Niggemann, M.; Katerkamp, A.; Pellmann, M.; Bolsmann, P.; Reinbold, J.; Cammann, K. *Sens. Actuators, B* **1996**, *34*, 328−333. (d) Abdelghani, A.; Chovelon, J. M.; Jaffrezic-Renault, N.; Veillas, C.; Gagnaire, H. *Anal. Chim. Acta* **1997**, *337*, 225−232.

(12) (a) Melendez, J.; Carr, R.; Bartholomew, D.; Taneja, H.; Yee, S.; Jung, C.; Furlong, C. *Sens. Actuators, B* **1997**, *38*−*39*, 375−379. (b) Melendez, J.; Carr, R.; Bartholomew, D. U.; Kukanskis, K.; Elkind, J.; Yee, S.; Furlong, C.; Woodbury, R. *Sens. Actuators, B* **1996**, *35*, 1−5.

(13) (a) Nelson, R. W.; Krone, J. R.; Jansson, O. *Anal. Chem.* **1997**, *69*, 4363−4368. (b) Krone, J. R.; Nelson, R. W.; Dogruel, D.; Williams, P.; Granzow, R. *Anal. Biochem.* **1997**, *244*, 124−132. (c) Owega, S.; Lai, E. P. C.; Bawagan, A. D. O. *Anal. Chem.* **1998**, *70*, 2360−2365.

(14) (a) Byahut, S.; Furtak, T. E. *Rev. Sci. Instrum.* **1990**, *61*, 27−32. (b) Futamata, M. *Appl. Opt.* **1997**, *36*, 364. (c) Nemetz, A.; Fischer, T.; Ulman, A.; Knoll, W. J. *Chem. Phys.* **1993**, *98*, 5912−5919. (d) Knobloch, H.; Brunner, H.; Leitner, A.; Aussenegg, F.; Knoll, W. J. *Chem. Phys.* **1993**, *98*, 10093−10095.

(15) Wink, T.; van Zuilen, S. J.; Bult, A.; van Bennekom, W. P. *Anal. Chem.* **1998**, *70*, 827−832.

(16) (a) Kubischko, S.; Spinke, J.; Bruckner, T.; Pohl, S.; Oranth, N. *Anal. Biochem.* **1997**, *253*, 112−122. (b) Buckle, P. E.; Davies, R. J.; Kinning, T.; Yeung, D.; Edwards, P. R.; Pollard-Knight, D. *Biosens. Bioelectron.* **1993**, *8*, 355−363. (c) Johne, B.; Hansen, K.; Mørk, E.; Holtlund, J. *J. Immunol. Methods* **1995**, *183*, 167−174.

(17) Brown, K. R.; Natan, M. J. *Langmuir* **1998**, *14*, 726−728.

(18) (a) Freeman, R. G.; Grabar, K. C.; Allison, K. J.; Bright, R. M.; Davis, J. A.; Guthrie, A. P.; Hommer, M. B.; Jackson, M. A.; Smith, P. C.; Walter, D. G.; Natan, M. J. *Science* **1995**, *267*, 1629−1632. (b) Grabar, K. C.; Smith, P. C.; Musick, M. D.; Davis, J. A.; Walter, D. G.; Jackson, M. A.; Guthrie, A. P.; Natan, M. J. *J. Am. Chem. Soc.* **1996**, *118*, 1148−1153. (c) Brown, K. R.; Fox, A. P.; Natan, M. J. *J. Am. Chem. Soc.* **1996**, *118*, 1154−1157. (d) Brown, K. R.; Keating, C. D.; Grabar, K. C.; Smith, P. C.; Botha, G. H.; Natan, M. J. In *Surface Modification of Polymeric Biomaterials*; Ratner, B. D., Castner, D. G., Eds.; Plenum Press: New York, 1996; pp 193−201. (e) Grabar, K. C.; Allison, K. J.; Baker, B. E.; Bright, R. M.; Brown, K. R.; Freeman, R. G.; Fox, A. P.; Keating, C. D.; Musick, M. D.; Natan, M. J. *Langmuir* **1996**, *12*, 2353−2361.

(19) (a) Turkevich, J.; Stevenson, P. C.; Hillier, J. *Discuss. Faraday Soc.* **1951**, *11*, 55−75. (b) Frens, G. *Nature Phys. Sci.* **1973**, *241*, 20−22. (c) Grabar, K. C.; Freeman, R. G.; Hommer, M. B.; Natan, M. J. *Anal. Chem.* **1995**, *67*, 735−743.

(20) Available on the Internet at rsb.info.nih.gov/nih-image/download.html.

(21) Goss, C. A.; Charych, D. A.; Majda, M. *Anal. Chem.* **1991**, *63*, 85−88.

(22) (a) Takemori, T.; Inoue, M.; Ohtaka, K. *J. Phys. Soc. Jpn.* **1987**, *56*, 1587−1602. (b) Hayashi, S.; Kume, T.; Amano, T.; Yamamoto, K. *Jpn. J. Appl. Phys.* **1996**, *35*, L331−L334. (c) Kume, T.; Nakagawa, N.; Hayashi, S.; Yamamoto, K. *Solid State Commun.* **1995**, *93* (2), 171−175. (d) Shchegrov, A. V.; Novikov, I. V.; Maradudin, A. A. *Phys. Rev. Lett.* **1997**, *78*, 4269−4272. (e) Holland, W. R.; Hall, D. G. *Phys. Rev. B* **1983**, *27*, 7765−7767. (f) Leung, P.-T.; Pollard-Knight, D.; Malan, G. P.; Finlan, M. F. *Sens. Actuators, B* **1994**, *22*, 175−180.

(23) Kreibig, U.; Vollmer, M. *Optical Properties of Metal Clusters*; Springer-Verlag: New York, 1995; pp 250−265.

(24) A more correct method for describing such a film may be an effective medium approximation such as Maxwell−Garnett theory26, which takes into account the thickness of the film and the volume fraction of the film components (Au and air, in this case). However, in either description, the film thickness is identically that of the particle diameter.

(25) Bohren, C. F.; Huffman, D. R. *Absorption and Scattering of Light by Small Particles*; John Wiley & Sons: New York, 1983; pp 130−154.

(26) (a) Hornyak, G. L.; Patrissi, C. J.; Martin, C. R. *J. Phys. Chem.* **1997**, *101*, 1548−1555. (b) Foss, C. A., Jr.; Hornyak, G. L.; Stockert, J. A.; Martin, C. R. *J. Phys. Chem.* **1994**, *98*, 2963−2971. (c) Maxwell−Garnett, J. C. *Philos. Trans. R. Soc. London A* **1904**, *203*, 385.